

ACCURACY COMPARISON TESTS ON ORTHO-RECTIFIED HIGH RESOLUTION SATELLITE IMAGES

C. Ioannidis, A. Katsigiannis

Dept. of Rural and Surveying Engineering, National Technical University of Athens, Athens 15780, Greece
cioannid@survey.ntua.gr

Commission I, WG I/5

KEY WORDS: Comparison, Accuracy, High resolution, IKONOS, Georeferencing, Geometric Modelling

ABSTRACT:

The aim of this paper is to study the impact of using various models for the determination of orientation parameters or georeferencing of high resolution satellite images, on the accuracy of the extracted DSM and orthorectified images. Empirical and physically based models are investigated: Rational Functions (RFC), Toutin's model and orbital parameter model, in which the satellite trajectories can be predicted or simulated by using the physical properties of the satellite orbits. Thus, orientation of every image of the scene can be determined with the Keplerian elements, the location and attitude of the platform.

A pair of IKONOS stereo Geo product images, at the north-western part of Athens, Greece, is used for the comparison tests. Twenty three ground points were measured by GPS, scattered all over the area covered by the images. Some of these points have been used for the determination of orientation parameters as GCPs, and the rest as check points. The process for DSM and ortho-image production, were done using: OrthoEngine^{SE} of PCI Geomatics software (using the RFM/RPCs with four different combinations of GCPs and the Toutin's model with 9 GCPs) and Leica Photogrammetry Suite (using RFM with two combinations of GCPs). The orbital model was used, in two data sets: the above IKONOS image pair and a SPOT5 image, in which 39 GSPs were available. Quality and accuracy controls on the ortho-rectified images, which were produced with all the above techniques, were made. The quality control was made by optical inspection of the whole area under study. Accuracy controls included the calculation and statistic analysis of the deviations of the measured on the orthoimages coordinates from the known accurate coordinates of the 14 check points. Also, accuracy controls were made between the ortho-images, which were produced from PCI and LPS, using various combinations of GCPs; the coordinate deviations were of the size of 1.2÷3.6 m. For each software package detailed conclusions are given for the functionality and the easiness in use, the accuracy and the completeness of the produced DSM, the errors of ortho-images and the improvement of accuracy using more control points.

1. INTRODUCTION

The launch and deployment of IKONOS satellite in September 24, 1999, was the first successful initiative for the operation of a series of high and mid resolution optical satellites for digital mapping through photogrammetric procedures. Today there are eight (8) high resolution satellites in orbit, with pixel resolution of their panchromatic images better than 2.5 meters (IKONOS, 1999; EROS A1, 2000; QuickBird, 2001; SPOT-5, 2002; OtbView 3, 2003; and FORMOSAT-2, 2004; IRS Cartosat-1, 2005; ALOS, 2006, which are soon expected to provide the market with stereo images), while it is already planned that seven (7) more satellites will be launched by the end of 2006 and six (6) more by the year 2010. Also, there are in orbit 14 mid resolution optical satellites (pixel 2.5 to 20 meters) and it is already announced that 10 more will be launched by the year 2010. All these satellites belong to 17 different countries of Europe, America and Asia.

The broad range of applications using these images is obvious and will be continuously increased in the following years as the number of satellites in orbit will be increasing and the size of their Ground Sample Distance will be decreased. Sensor orientation modeling for the geo-referencing of the satellite images is a prerequisite for the production of DSM and orthoimages or even for the stereo-restitution. It is practically the only difference in comparison with the processing of airborne digital images. This relation between image and ground

coordinates can be achieved with two types of models (Di et al, 2003; Niu et al, 2004; Toutin, 2004):

- empirical models or non-physically based models, including DLT or self calibration DLT, 3D affine transformation, multiquadric functions, mapping polynomials and Rational Function Model (RFM)
- physically based models, which include the rigorous sensor model, generic sensor model, and replacement sensor model.

Today, many Digital Photogrammetric Workstations (DPW) have software modules for georeferencing of almost all satellite sensors, which use one or more of the above mentioned models. It has been shown that for high resolution satellite scenes the accuracies of products, such as orthoimages and DSM derived with RFM can meet the accuracies of the rigorous approach, if some improvements are made by ground control information (Valadan and Sadeghian, 2003; Lehner et al, 2005). Refinement of the RPCs can be based on a large number of GCPs or on the use of a polynomial correction in either the image space or object space (Di et al, 2003; Hanley and Fraser, 2004).

In this paper the impact of using RFM and other empirical models as well as physically based models (Toutin's model and an orbital parameter model) for the determination of the orientation elements of a pair of IKONOS stereo Geo product images, on the accuracy of the extracted DSM and orthorectified images using two DPWs (OrthoEngine^{SE} of PCI Geomatics and Leica Photogrammetric Suite) is investigated.

2. ORIENTATION MODELS

2.1 Empirical models

Several simple or more complex models have been proposed, based on polynomial equations (Valadan and Sadeghian, 2003; Niu et al, 2004); yet, the RFM approach is the most integrated and common solution in the category of empirical models. The RFM is a generalized sensor model, which allows the user to deal with various sources of imagery without having to know about details of interior and exterior orientation of the sensor system. It is best appropriate for satellites such as IKONOS, where position, velocity vectors and angular rates of the platform have not been provided.

The RFM model uses a pair of ratios from two polynomials (Equation 1) to transform a point from the object space to the image space. The coefficients of the RFM are called Rational Polynomial Coefficients (RPCs) or Rational Function Coefficients (RFCs). It should be mentioned that a normalization procedure has to be done beforehand so that numerical stability will be achieved.

$$r_n = \frac{p1(X_n, Y_n, Z_n)}{p2(X_n, Y_n, Z_n)} \quad c_n = \frac{p3(X_n, Y_n, Z_n)}{p4(X_n, Y_n, Z_n)} \quad (1)$$

where: r_n , c_n - the normalized image coordinates,
restricted to $[-1, +1]$ interval, and
 X_n , Y_n , Z_n - the normalized geodetic (or geographic – ϕ_n , λ_n , h_n)
coordinates of a point.

The polynomial P_i ($i = 1, 2, 3, 4$) is a third-order rational function with a 20-term polynomial that, and has the following form:

$$\begin{aligned} p_i(X_n, Y_n, Z_n) = & a_1 + a_2 X_n + a_3 Y_n + a_4 Z_n + a_5 X_n Y_n + a_6 X_n Z_n + \\ & + a_7 Y_n Z_n + a_8 X_n^2 + a_9 Y_n^2 + a_{10} Z_n^2 + a_{11} X_n Y_n Z_n + a_{12} X_n^3 + \\ & + a_{13} X_n Y_n^2 + a_{14} X_n Z_n^2 + a_{15} X_n^2 Y_n + a_{16} Y_n^3 + a_{17} Y_n Z_n^2 + \\ & + a_{18} X_n^2 Z_n + a_{19} Y_n^2 Z_n + a_{20} Z_n^3 \end{aligned} \quad (2)$$

Although RPCs/RFM do not describe sensor parameters explicitly, they are used because it is simple to implement and perform transformations very rapidly.

The determination of the initial values of the RPCs can be made using two different approaches (Zhou and Li, 2000; Grodecki and Dial, 2003):

- terrain independent – utilizes the satellite on-board orientation, which includes orbital parameters and attitude data (from instruments such as GPS, INS and star trackers which are on the satellite) in generating enough transformation anchor points
- terrain dependent – computes the unknowns of the polynomial functions using a huge number of ground control points (GCPs), smoothly distributed in the whole area of the image and represent well the relief of the area.

2.2 Physically based models

There are two robust types of sensor models for pushbroom satellite images:

- orbital parameters model, using the Kepler elements and
- state vectors model, which calculates the orbital parameters directly by using the position vector.

In this paper the results of the application of two rigorous models, that have been suggested during the last 15 years, are examined and tested. In both of the models the observation equations represent the collinearity condition appropriately adjusted in order to be valid for the satellite images. The first is the 3D parametric model developed by Toutin at the Canada Centre for Remote Sensing (named ‘Toutin’s model’), which has been embodied into OrthoEngine^{SE} software of PCI Geomatics. It is an integrated and unified model to geometrically process multi-sensor images. It has been applied to visible and infra-red data as well as radar data. The final equations of the model include the different distortions relative to the global geometry of viewing, that is the distortions caused by the platform (position, velocity, orientation), the sensor (orientation angles, instantaneous FOV, detection signal integration time), the earth (geoid, ellipsoid, relief) and the cartographic projection (ellipsoid-cartographic plane).

Four processing steps are followed:

- Pre-processing: determination of approximate value for each parameter of the model
- Acquisition of data: measurement of the 3D cartographic coordinates of GCPs and their 2D image coordinates
- Processing of the model: computation of the initial values and refinement of the parameters of the 3D model
- Products: generation of DSM and orthoimages.

Details about the mathematic model and its parameters are given in (Toutin, 2003).

The second model was developed at Purdue University (Makki, 1991). For each GCP the following equation (3) is created, which is a function of time for the acquisition of each image of the satellite scene. In this equation both sensor parameters, that is focal length, principal point location, lens distortion, line rate, detector (pixel) size, and platform parameters, that is location X , Y , Z , attitude roll, pitch, yaw, Kepler orbit elements (semi-major axis a , inclination i , argument of perigee ω , eccentricity e , true anomaly f and right ascension of ascending node Ω) are included.

$$\begin{bmatrix} 0 \\ y \\ -f \end{bmatrix} = \lambda \cdot M_t \cdot M_a \cdot M_b \cdot \begin{bmatrix} X \\ Y \\ Z \end{bmatrix} - \begin{bmatrix} 0 \\ 0 \\ R_s \end{bmatrix} + \begin{bmatrix} \Delta X \\ \Delta Y \\ \Delta Z \end{bmatrix} \quad (\text{Equation 3})$$

where:

M_b – the result of multiplication of three angle-matrices, which are created by Ω ($a_1=\Omega-\omega_c t$), inclination i ($a_2=i+90^\circ$) and ω / true anomaly ($a_3=\omega+f+90^\circ$)

$$M_a = M_{\Delta\kappa} M_{\Delta\phi} M_{\Delta\omega}, \quad \text{with: } \Delta\omega = \omega_0 + \omega_1 \Delta t + \omega_2 \Delta t^2 \\ \Delta\phi = \phi_0 + \phi_1 \Delta t + \phi_2 \Delta t^2 \\ \Delta\kappa = \kappa_0 + \kappa_1 \Delta t + \kappa_2 \Delta t^2$$

R_s - the vector connecting the origin of the geocentric system with each image of the satellite scene

$$R_s = a(1-e \cos E), \quad \text{with } E: \text{eccentric anomaly}$$

ΔX , ΔY , ΔZ – corrections of the coordinates

$$\Delta X = X_o + X_1 \Delta t + X_2 \Delta t^2$$

$$\Delta Y = Y_o + Y_1 \Delta t + Y_2 \Delta t^2$$

$$\Delta Z = Z_o + Z_1 \Delta t + Z_2 \Delta t^2$$

From the equation (3) the two observation equations (4) are derived, which include up to 28 unknowns: the 6 Kepler elements, 9 attitude and 9 location parameters, 3 satellite pointing corrections and the focal length of the sensor.

$$F_x = \frac{R_{11} \cdot (X_i - r_{31} \cdot R_{31} - \Delta X_i) + R_{12} \cdot (Y_i - r_{32} \cdot R_{31} - \Delta Y_i) + R_{13} \cdot (Z_i - r_{33} \cdot R_{31} - \Delta Z_i)}{R_{31} \cdot (X_i - r_{31} \cdot R_{31} - \Delta X_i) + R_{32} \cdot (Y_i - r_{32} \cdot R_{31} - \Delta Y_i) + R_{33} \cdot (Z_i - r_{33} \cdot R_{31} - \Delta Z_i)}$$

$$F_y = y + \frac{R_{21} \cdot (X_i - r_{31} \cdot R_{31} - \Delta X_i) + R_{22} \cdot (Y_i - r_{32} \cdot R_{31} - \Delta Y_i) + R_{23} \cdot (Z_i - r_{33} \cdot R_{31} - \Delta Z_i)}{R_{31} \cdot (X_i - r_{31} \cdot R_{31} - \Delta X_i) + R_{32} \cdot (Y_i - r_{32} \cdot R_{31} - \Delta Y_i) + R_{33} \cdot (Z_i - r_{33} \cdot R_{31} - \Delta Z_i)} \quad (\text{Equations 4})$$

For the operation and checking of this model, a special software (named 'ORBITALGEN') in MatLab environment is written at the Laboratory of Photogrammetry of National Technical University of Athens. First an application of this software was made using a SPOT-5 image, for which accurate ephemeris data are available; consequently, the Kepler elements and the sensor's focal length were considered to be known, and the unknowns were eliminated in 18. At the study site 20 GCPs and 19 check points (ICPs) existed. After several adjustments it was proved that the 2nd order terms at the polynomials of attitudes and locations were not significant; so, finally, only 12 unknowns were determined. The discrepancies at the ICPs coordinates were:

$\text{rms (DX)} = 0.7 \text{ pixels}, \quad \text{rms (DY)} = 2 \text{ pixels.}$

3. PRODUCTION OF DSM AND ORTHO-RECTIFIED IMAGES

3.1 Description of the data

The original data for the quality and accuracy control of the produced ortho-rectified images, after the application of the above mentioned orientation models, were a pair of IKONOS stereo Geo and Geo Ortho Kit product images. The study site is an area at the north-western part of Athens, Greece. Three quarters of this site is covered by dense urban residential environment and the rest, in the middle of its northern part, is a typical semi-rural environment with scattered agricultural land. The area is comparatively flat, with an elevation range of 180m; the lower altitudes exist at the south-western part and the higher at the north-eastern part.

Twenty three ground points, scattered all over the site, were measured by GPS with an accuracy of approximately 20cm for each coordinate. Some of these points have been used as GCPs, and the rest as independent check points (ICPs). Figure 2 shows the distribution of these points in a ortho-rectified image. The processing of the satellite images was made at two DPWs, so that the alternatives procedures and the operation of each one would be investigated and their products would be compared.

3.2 Orthoimage production by the PCI Geomatics

IKONOS Geo Ortho Kit data were processed at module OrthoEngine^{SE} of PCI Geomatica v.9.1. This software provides two methods of processing the IKONOS data:

- "Rational Functions" (RFM), with three options at the menu "Select Rational Functions": "Compute from GCPs" in the case that no initial values for the RPCs exist (required 40 GCPs and "Satellite Models" software package), "Extract from Image File" in the cases that the RPCs will be used as they are given from Space Imaging (required "IKONOS Models" software package) or refinement of the RPCs will be made using even one GCP
- "Satellite Orbital Modelling" (Toutin's model), through the selection of "High Resolution" at the relevant menu.

With the exception of the case "Compute from GCPs" (calculation of the initial RPCs from GCPs), all other

procedures were applied for our controls. In particular, solutions were made by using:

- Rational Function Model with the original RPCs, which accompany each image
- RFM with refined RPCs by using 3 GCPs (that lay at the perimeter of the site – points 1, 4 and 21 on Figure 2)
- RFM with refined RPCs by using 6 GCPs (GCPs of the previous solution plus the points 10, 11and 12)
- RFM with refined RPCs by using 9 GCPs (GCPs of the previous solution plus the points 9, 22 and 23)
- Toutin's model using 9 GCPs.

The same photogrammetric procedure was followed for all the above products:

- creation of epipolar images
- extraction of DSM automatically, using 8m pixel sampling interval; Figure 1 shows the DSM extracted by using RFM/original RPCs
- orthoimage production.

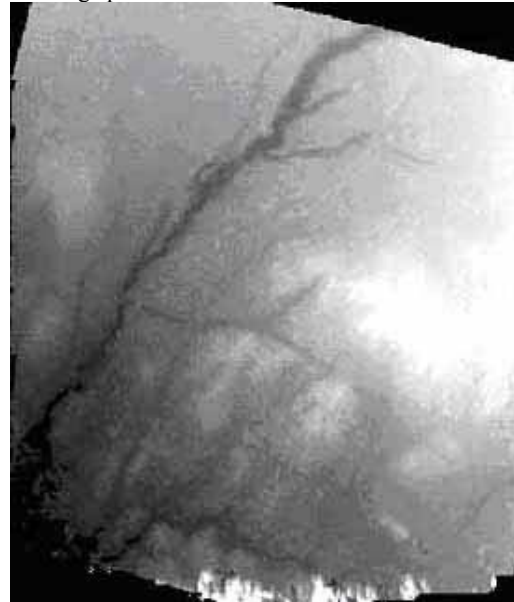


Figure 1. DSM of the site, in raster format

3.3 Orthoimage production by the LPS

IKONOS Geo Ortho Kit data were processed at OrthoBase^{SE} of ERDAS IMAGINE v8.6, which now is included into the module Leica Photogrammetric Suite^{SE} (LPS). With this software, images derived from analog or digital airborne cameras and spaceborn images of various satellites (IKONOS, IRS, QuickBird, SPOT, EROS etc) can be processed. Georeferencing of the satellite images can be achieved only by using RFM/RPCs, since the software does not contain any rigorous orientation model. So, the following controls were made:

- use of Rational Function Model with the RPCs which accompany each image
- use of RFM with refined RPCs derived from 4 GCPs
- use of RFM with refined RPCs derived from 4 GCPs.

Epipolar images are not necessary for the DSM extraction, while a variety of strategies is provided, whose selection was proved to have an impact on the accuracy of the derived altitudes. For all the above controls a DSM cell size of 10m was selected. Figure 2 shows the ortho-rectified image derived from the nadir-looking satellite image, using the RFM/original RPCs.

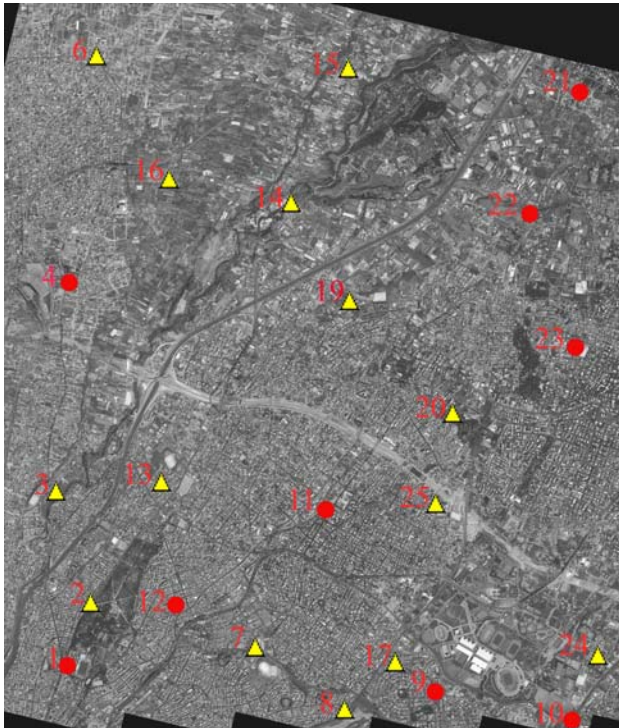


Figure 2. Ortho-rectified image, produced by LPS, where the measured points are shown:
● GCPs ▲ ICPs

3.4 Results from orbital parameters model

An application of ‘ORBITALGEN’ software, which was developed at the Laboratory for the determination of rigorous orbital model parameters, was made, using IKONOS Geo product stereo-images data. The most difficult part is the estimation of satisfactory initial values for the unknowns Keplerian elements, since there are no satellite on-board ephemeris data for IKONOS. Still on the metadata file, that comes together with the images, the date and the exact time of the image collection is mentioned. Through these data and using WinOrbit^{SE} software, the vectors for the location and speed of the satellite can be determined and consequently the Kepler elements can be calculated.

Several solutions were made by changing the number of unknowns of the model, which gave a variety of results:

- The system does not give a solution when all 28 unknowns are used (full model)
- A convergence of the system can be achieved only after taking out the coefficients of the 2nd order related to time (t) at the polynomials of attitudes and locations; yet, some deviations of several pixels were observed at the coordinates of ICPs
- Best results are achieved when the system has only 6 unknowns: the coefficients of 1st order for the time (t) at the polynomials of attitudes and locations. The root mean square (rms) of deviations in horizontal coordinates of 14 ICPs is 1.5±2.5 pixels, although there is uncertainty in the determination of the coefficients in the Y and Z axes.

Consequently, there is uncertainty concerning the possibility of the model’s convergence for IKONOS data, which depends on the number of unknowns that will participate to the solution and on the good determination of initial values for the Keplerian elements.

4. COMPARISON TESTS

4.1 Quality control of ortho-rectified images

Orthoimages were produced from both IKONOS images of the stereo-pair, for all solution of the geometric models made at the two DPWs (PCI and LPS). Quality control was the first control applied to those orthoimages and it was made by a separate optical inspection for each one.

Derived conclusions are similar for all orthoimages produced at both DPWs from the nadir-looking image:

- they are especially clear images, with natural colors without any problem from radiometric aspect
- no distortions are found, not even at high constructions, such as the very tall buildings that exist in the urban part of the site, the multilevel road junctions etc; an example is given at Figure 3(a), where the road intersection is shown accurately.

On the contrary, distortions are detected at the very tall constructions in all ortho-rectified images that were produced from the backward-looking image; Figure 3(b) shows an example. The size of the problem varies according to the orientation model used, without having any better products by PCI or by LPS.



Figure 3. Orthoimages of a multilevel road junction, produced
 (a) the nadir-looking and by (b) the backward-looking image

4.2 Accuracy tests

Accuracy controls refer to the final product of the photogrammetric procedure, the ortho-rectified images. In this way both the errors of the geometric model for the images’ georeferencing and of the automatic DSM extraction can be considered. For each orthoimage the absolute and relative errors of the (X, Y) coordinates of the same 14 ICPs were determined; also the errors in distances between the ICPs, and the relative deviations between orthoimages were determined.

Table 1 shows the absolute and relative errors in the object space, for the five solutions at the PCI and for the three solutions at LPS, which mentioned above (for the cases PCI_RPC_n and LPS_RPC_n, n is the number of GCPs which was used for the refinement of the RPCs). The systematic error that exists especially at the X coordinate, after the application of the RFM with the original RPCs, is diminished to a great extent by the use of a few GCPs for the refinement of the RPCs. This is more obvious in the solutions with the PCI, where a larger systematic error exists; at the solutions with the LPS the errors using the original RPCs are smaller, but the systematic error in rms(DX) remains large even after the use of the 9 GCPs. However, in all solutions with RFM as orientation model, the errors remain larger than 1 GSD, even without their systematic part ($\sigma_{DX} - \sigma_{DY}$).

Case	rms (DX) m	rms (DY) m	max (DX) m	max (DY) m	$\sigma_{(DX)}$ m	$\sigma_{(DY)}$ m	rms (DS) m
PCI RPC_0	6.03	1.99	7.25	2.88	0.75	1.86	1.99 [$\sigma_{X,Y} = 1.41$]
PCI RPC_3	2.75	1.72	4.68	3.11	1.29	1.16	2.18 [$\sigma_{X,Y} = 1.54$]
PCI RPC_6	2.01	1.19	3.15	2.94	1.02	1.19	2.29 [$\sigma_{X,Y} = 1.62$]
PCI RPC_9	1.84	1.10	3.10	2.04	1.24	1.03	2.32 [$\sigma_{X,Y} = 1.64$]
PCI Tутин 9	1.81	1.52	3.77	2.48	1.68	1.50	2.05 [$\sigma_{X,Y} = 1.45$]
LPS RPC_0	4.82	1.79	6.14	2.93	1.04	1.63	2.21 [$\sigma_{X,Y} = 1.49$]
LPS RPC_4	3.96	1.38	5.19	2.35	0.94	1.36	2.29 [$\sigma_{X,Y} = 1.62$]
LPS RPC_9	3.66	1.43	4.17	2.81	1.37	1.16	1.75 [$\sigma_{X,Y} = 1.24$]

Table 1. Absolute and relative errors in the object space on 14 ICPs measured on the orthoimages derived by the PCI and LPS

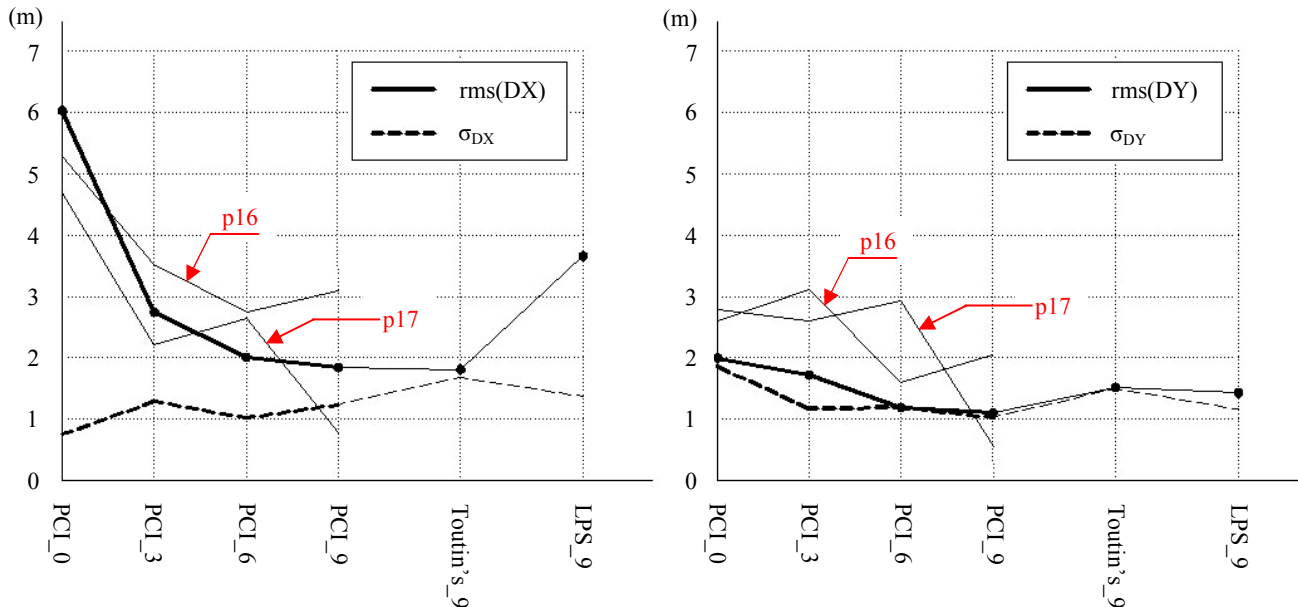


Figure 4. Statistical results computed from the difference between the orthoimages and the GPS measurements on 14 ICPs

The relative errors, as they appear from the standard deviations and the distance errors, are for each DPW practically the same regardless of the number of GCPs used. Toutin's model application gives almost the same results with those of the RFM with the same number of GCPs used. Figure 4 shows in diagrammes (on the left for X axis and on the right for Y axis) the above-mentioned conclusions. Also, the curves of absolute errors for two ICPs (with code numbers '16' and '17') are given for the RM solutions at PCI. The general conclusions are valid exactly for point '16', which in all cases lies outside of the perimeter of the GCPs which used each time. The behavior of point '17' depends on whether it lies inside or outside of the perimeter of the GCPs or whether it is close to a GCP.

It is worth mentioning that the differences in the 14 ICPs coordinates measured on the two orthoimages produced at PCI and LPS with RFM/RPCs using 9 GCPs, are large:

$$\text{rms (DX)} = 3.62 \text{ m}, \text{ max (DX)} = 4.76 \text{ m}$$

$$\text{rms (DY)} = 1.47 \text{ m}, \text{ max (DY)} = 2.06 \text{ m}$$

On the contrary, the differences of the coordinates are small in the comparisons between orthoimages produced at the same DPW (the PCI) when a different number of GCPs are used:

- using 3 and 6 GCPs: $\text{rms}(DX)=0.96 \text{ m}$, $\text{rms}(DY)=1.63 \text{ m}$
- using 6 and 9 GCPs: $\text{rms}(DX)=1.70 \text{ m}$, $\text{rms}(DY)=0.66 \text{ m}$.

The existence of a systematic part in the error results after the application of RFM/refined RPCs, regardless the number of GCPs used, makes the further processing of the images

attractive through simple polynomial models, before any other photogrammetric processing (e.g. DSM extraction etc). The three following models were applied, using additional GCPs different from those that were used for the geo-referencing of the images with the RFM/RPCs:

- Translation in object space (2 unknowns – at least 1 GCP)
- Scale and translation (4 unknowns – at least 2 GCPs):

$$X' = a_0 + a_1 X \quad Y' = b_0 + b_1 Y \quad (\text{Equations 5})$$
- Affine in object space (6 unknowns – at least 3 GCPs):

$$X' = a_0 + a_1 X + a_2 Y \quad Y' = b_0 + b_1 X + b_2 Y \quad (6)$$

Table 2 shows the results (absolute errors, systematic part, relative errors) for various combinations of solutions. The observed improvements in accuracy are rather impressive since all these transformations are already included in the polynomials of the Rational Functions. The application of a simple translation seems to be sufficient for the elimination of the remaining systematic errors when a few GCPs are used (3 ñ 6) in the RFM/RPCs. However, in all cases, the best results were derived from the combined application of RFM and affine transformation. It is worth mentioning that the absolute errors become less than 1 GSD by using 9 GCPs, from which one only is enough for the refinement of the RPCs and the rest for the determination of affine transformation parameters (at least 6 GCPs must be available for this processing).

Case (14 cp)	RMS (DX) m	RMS (DY) m	Mean (DX) m	Mean (DY) m	$\sigma_{(DX)}$ m	$\sigma_{(DY)}$ m
0	6.03	1.99	-5.74	-0.67	0.75	1.86
3-A	2.75	1.72	-2.33	-1.23	1.29	1.16
3-B	0.99	2.43	0.69	1.34	0.64	1.98
3-C	1.80	1.99	-1.11	-1.10	1.39	1.63
3-D	1.54	1.19	-0.81	0.49	1.30	1.08
6-A	2.01	1.19	-1.66	0.06	1.02	1.19
6-B	1.38	1.27	-0.14	0.03	1.36	1.27
6-C	1.08	0.84	-0.63	0.72	0.86	0.38
6-D	1.17	0.37	0.49	-0.32	1.05	0.16
6-E	1.59	1.69	-0.81	1.06	1.35	1.28
9-A	1.84	1.10	3.10	2.04	1.24	1.03
9-B	1.55	1.44	-1.29	-0.21	0.71	1.43
9-D	1.17	0.31	-0.85	0.13	0.75	0.28
9-E	1.76	0.97	-1.28	0.39	1.11	0.88
9-F	0.96	0.37	-0.57	-0.23	0.75	0.28

Table 2. Errors on the orthoimages produced by using various empirical geo-referencing models

where (with $n = 0, 3, 6, 9$; that is the number of known GCPs):

n-A : refinement of RPCs using n GCPs

n-B : refined RPCs using ($n-3$) GCPs plus translation (using the 3 new GCPs)

n-C : refined RPCs using ($n-3$) GCPs plus translation and scale

n-D : refined RPCs using ($n-3$) GCPs plus affine transformation

n-E : original RPCs plus affine transformation (using n GCPs)

n-F : refined RPCs using 3 GCPs plus affine transformation

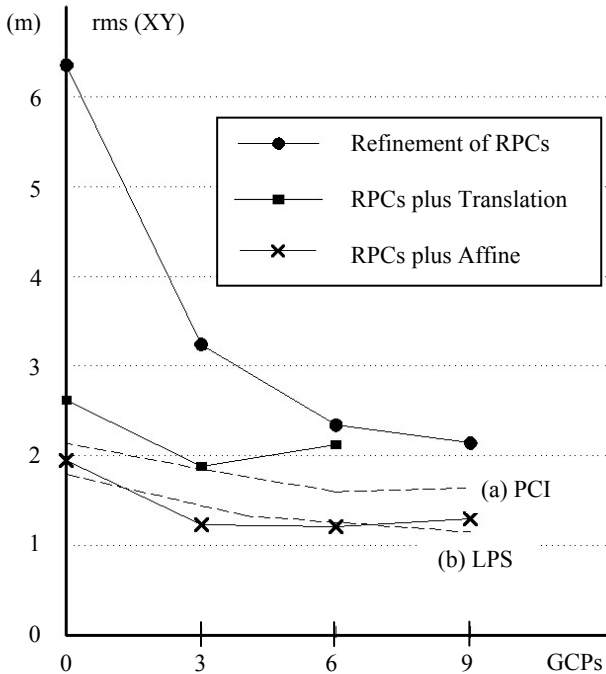


Figure 5. Orthoimage accuracy variation according to the image orientation model and the increase of GCPs number

Figure 5 shows what impact the translation and the affine transformations has on the orthoimage accuracy; the errors of ICPs after the application of the RFM and before any other procedure (DSM extraction and orthoimage production) are shown with dashed line.

5. CONCLUSIONS

The application both of the empirical and the physically based models for the orientation of IKONOS images, under certain circumstances and with the aid of ground control, is proved to be able to return an accuracy of the produced orthoimages through automatically extracted DSM, better than 1 GSD (1m). In the cases that more than 6 GCPs are known, the best results are achieved by applying :

- the RFM with refinement RPCs using only 1 GCP, and
- an affine transformation using the rest of the GCPs.

The use of an orbital model may result to an unstable system.

The two DPWs, that have been used, produced orthoimages of similar quality, which differ in accuracy. The differences are due mostly to the accuracy of the extracted DSM; an overestimation of the altitudes is noticed at the PCI, while an underestimation is noticed at LPS.

REFERENCES

- Di, K., Ma, R., Li, R., 2003. Rational functions and potential for rigorous sensor model recovery. *Photogrammetric Engineering and Remote Sensing*, 69(1), pp. 33-41.
- Grodecki, J., Dial G., 2003. Block adjustment of high-resolution satellite images described by rational polynomials. *Photogrammetric Engineering and Remote Sensing*, 69(1), pp. 59-68.
- Hanley, H.B., Fraser, C.S., 2004. Sensor orientation for high-resolution satellite imagery: Further insights into bias-compensated RPCs. In: *The International Archives of the Photogrammetry, Remote Sensing and Spatial Information Sciences*, Istanbul, Turkey, Vol. XXXV, Part B1, pp. 24-29.
- Lechner M., Mueller R., Reinartz P., 2005. DSM and orthoimages from QuickBird and IKONOS data using Rational Polynomial Functions. In: *International Archives of Photogrammetry and Remote Sensing*, Hannover, Germany, Vol. XXXVI, Part 1/W3, unpaginated CD-ROM.
- Makki, S., 1991. Photogrammetric reduction and analysis of real and simulated SPOT imageries. *Ph.D. thesis. Purdue University, West Lafayette*.
- Niu, X., Wang, J., Di, K., Lee, J-D., Li R., 2004. Geometric modelling and photogrammetric processing of high-resolution satellite imagery. In: *The International Archives of the Photogrammetry, Remote Sensing and Spatial Information Sciences*, Istanbul, Turkey, Vol. XXXV, Part B4, pp. 689-694.
- Toutin, T., 2003. Error tracking in IKONOS geometric processing using a 3D parametric model. *Photogrammetric Engineering and Remote Sensing*, 69(1), pp 43-51.
- Toutin, T., 2004. Geometric processing of remote sensing images: Models, algorithms and methods. *International Journal of Remote Sensing*, 25(10), pp. 1893-1924.
- Valadan Zanj, M.J., Sadeghian. S., 2003. Orbital parameter modeling accuracy testing of Ikonos Geo image. *Photogrammetric Journal of Finland*, 18(2), pp. 70-80.
- Zhou, G., Li, R., 2000. Accuracy evaluation of ground points from IKONOS high-resolution satellite imagery. *Photogrammetric Engineering and Remote Sensing*, 66(9), pp. 1103-1112.